SIGNAL PROCESSING IN SPACE-SURFACE BISTATIC SYNTHETIC APERTURE RADAR

M.Cherniakov, R.Saini, M. Antoniou, Rui Zuo, J.Edwards

Department of Electronic, Electrical and Computer Engineering
University of Birmingham, Edgbaston, Birmingham, United Kingdom, B15 2TT
Email: sainir@bham.ac.uk

1 INTRODUCTION

Space-Surface Bistatic Synthetic Aperture radar (SS-BSAR) consists of a space-borne transmitter and a receiver mounted on an aircraft (Figure 1)[1]. One of the features of the SS-BSAR architecture shown in Figure 1 is its asymmetric structure, which is in contrast to a more usual BSAR configuration where the transmitter and receiver are moving along collinear trajectories.

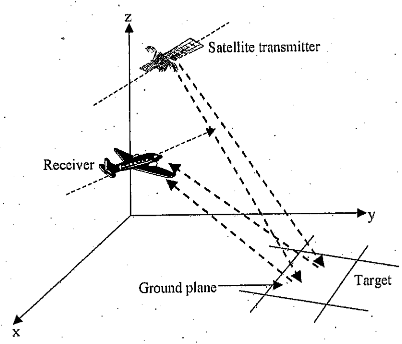

Figure 1: SS-BSAR with NCT

Over the last decade SS-BSAR, in particular SS-BSAR with non-cooperative transmitters (NCT) has generated a lot of interest [2-5]. This technology utilises existing transmitters of broadcasting, communications and navigation satellites, as well as space-borne radar.

In this paper we consider SS-BSAR with an airborne receiver, utilising microwave emissions from a global navigation satellite system (GNSS) as the ranging signal; in particular, we will be using a GLONASS navigation satellite for experimentation. It should be noted that although we are considering a particular satellite system, the structure and main parameters of the radar system are generic and could be used with different space-borne transmitters.

Our previous publications [2-5] have discussed various aspects of SS-BSAR. The resolution of such a system was presented in [2], the power budget and the different sources of interference present in SS-BSAR being considered in [3]. The hardware developed to study SS-BSAR experimentally was discussed in [4] and, in [5], the issue of signal synchronisation was considered and experimental verification using GLONASS satellites was reported. Also a SS-BSAR imaging algorithm was proposed and imaging results using a stationary satellite signal imitator were given.

This paper extends our previously published work by considering imaging using a real satellite. It proposes a suitable imaging algorithm and presents the image obtained using a real satellite. A comparison is made between the images obtained using the satellite and using a satellite signal imitator.

2 SS-BSAR IMAGING

2.1 Signal Processing Algorithm

Figure 2 shows the system geometry. The navigation satellite is positioned as shown, the angles θ_A and θ_E being, respectively, the azimuth and elevation angles of the satellite relative to the receiver which is moving in the (0,y, z) plane, parallel to the y axis. The observation area is located in the (x,y,0) plane. The bistatic angle β is the angle between the target illumination and echo propagation paths. As per the definition of bistatic radar, the transmitter and receiver are separated by distance L. The distance from transmitter to target is R_T and the distance from receiver to target is R_R. As the transmitter and receiver are in motion, R_T, R_R and L are functions of time.

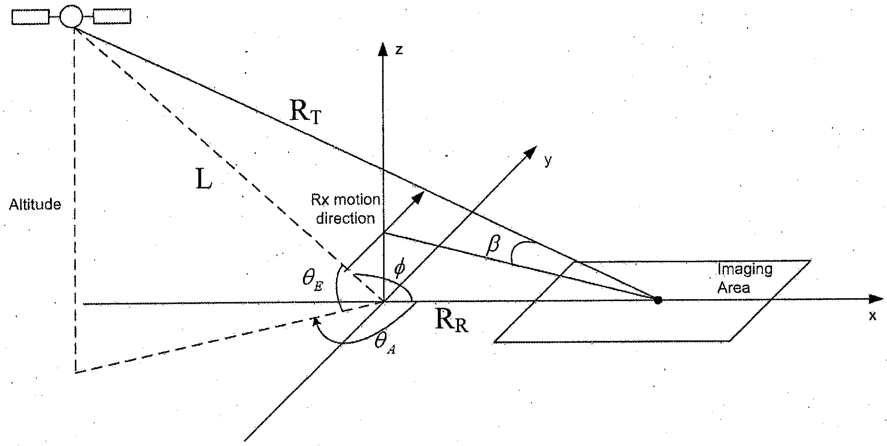

Figure 2: Three-dimensional system geometry

The proposed signal-processing algorithm for SS-BSAR is a modification of the standard Range-Doppler Algorithm (RDA), see Figure 3. The only difference between the standard RDA and the proposed algorithm is in the design of azimuth filter, which is derived from the instantaneous bistatic triangle formed by the transmitter, receiver and the target as shown in figure 2.

The following assumption are made in developing the algorithm for the work in progress:

- Moderate aperture length is considered (30 m for experimentation) allowing the range migration step of the normal RDA to be ignored.
- Targets at short ranges are considered (maximum range ~ 600 metres).
- For experimentation, a two-channel receiver is considered: the radar channel used for receiving the reflected signal from the observation area and the heterodyne (reference) channel receiving a signal directly from the satellite. The radar channel antenna is mounted on a flight imitator for array synthesis but, at this stage, the heterodyne channel is stationary (see Figure 4).

The different components of the modified RDA algorithm are shown below:

Reference Signal: For the considered system of satellites (GNSS), one cannot directly correlate the heterodyne channel with the radar channel. This is explained as follow:

The signal from the GNSS is the superposition of two signals; namely the C/A code and the P-code, the spectra of which overlap. The P-code (5.11 MHz bandwidth) of the GLONASS satellite is used for the purpose of imaging, as it provides adequate range resolution (30 m in the quasi-bistatic case) and is no longer encrypted. The C/A code has 10 times narrower bandwidth compared with the P-code. Therefore, if the heterodyne channel is directly correlated with the radar channel, the P-code will be masked by C/A code at the output of the multi-channel correlator. Even if the C/A code of the desired satellite is filtered out in the heterodyne channel, the signal correlation properties are degraded by the C/A code of the interfering satellites. A detailed explanation of this self-interference is given in [5]. It was also shown that, if the radar channel signal is correlated with a locally generated signal containing only the P-code, the effect of the C/A could be suppressed.

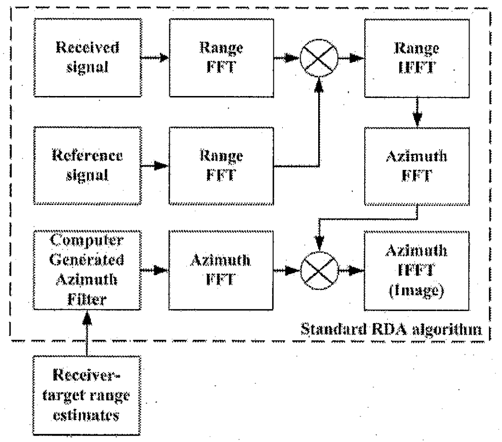

Figure 3:SS-BSAR proposed algorithm

The locally generated P-code needs to be synchronised (in time and Doppler) with the heterodyne channel P-code signal before it is correlated with the radar channel signal (see Figure 4). This is to maintain the phase coherence between the radar channel and the locally generated P-code. Successful synchronisation using a GLONASS satellite has been reported in [5].

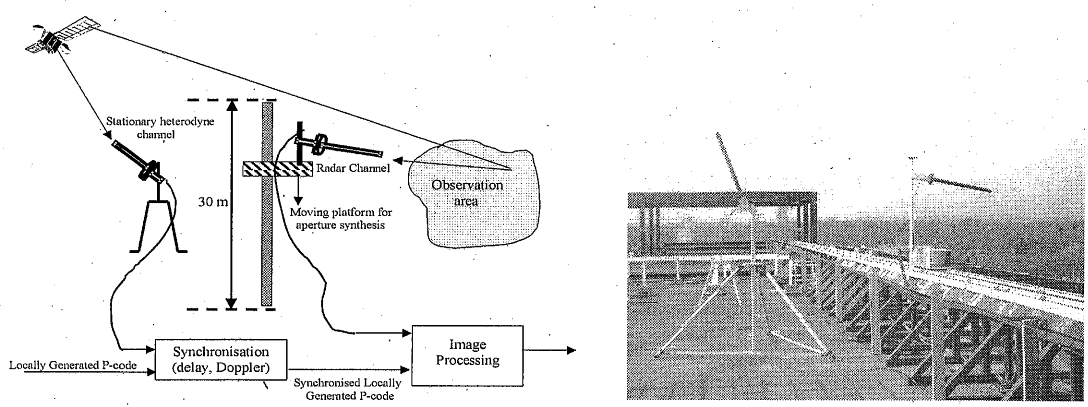

Figure 4: Experiment set-up

Range Compression: Figure 5 shows the simplified two-dimensional diagram forming the bistatic triangle. As mentioned earlier the locally generated signal is synchronised to the heterodyne channel signal. Therefore after range correlation, a target at distance R_R from the receiver is located by the radar at the range $R_T' + R_R(u)$, where $R_T' = R_T(t) - L(t)$ and u is the slow time. For each range bin, R_T' is constant. This is due to negligible angular variation of the satellite during the time of flight and the moderate aperture length.

Azimuth Compression: Doppler shift is evident along different paths in the bistatic triangle. As we are considering a stationary heterodyne channel and targets at short ranges, the Doppler shifts due to satellite motion (fs) in the heterodyne channel and transmitter-to-target paths are similar. The azimuth phase variation is due to the receiver motion only (R_R variation). Therefore in order design an appropriate azimuth filter, for each range bin we need to find R_R from $R_T' + R_R$. This can be estimated by solving the bistatic triangle of Figure 5, which in turn requires estimates of L(t) and φ. The synchronisation algorithm tracks the satellite in delay and hence provides an estimate of L. The angle φ can be measured using an off-the-shelf GNSS receiver, which provides the satellite's coordinates (azimuth and elevation angles).

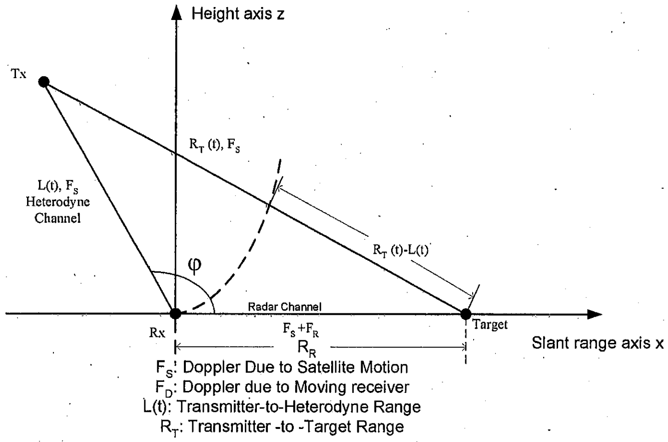

Figure 5: Two-dimensional system geometry

2.2 Experimental Set-up

An experiment was conducted using the flight imitator installed on the rooftop of a five-storey building (Figure 4). A GLONASS satellite was selected in such way that the 'transmitter-receiver-target' topology corresponds to a quasi-bistatic case. The satellite selection was carried out by using a commercial GNSS receiver. Table1 shows the different experimental parameters of Figure 2

Frequency Channel	10 (1607.625 MHz)
θ_A	178.4914 degrees
θ_E	11.3558 degrees
β	~11 degrees
Satellite Altitude	~23000 km
Aperture length	30 meters
Receiver velocity	0.6 m/sec
Integration Time	45 second

Figure 6(a) shows the image obtained using a real satellite, whereas Figure 6 (b) presents the image obtained using a satellite signal imitator, also in a quasi-monostatic configuration. The radar images have been rescaled and superimposed on an aerial photograph of the same region for comparison.

Comparison of figures 6(a) and 6(b), shows a high level of similarity, suggesting that the system is functioning properly. It is seen that a building (at range 250m) and part of the structure of a greenhouse (in the range interval 350-400m) have been clearly identified in both images. The grassy areas appear as shades of blue (low intensity) as expected.

3 CONCLUSIONS

This paper considered the SS-BSAR with an airborne receiver, utilising microwave emissions from global navigation satellite system (GNSS) as the ranging signal. GLONASS satellite was used for experimentation.

An SS-BSAR imaging algorithm was proposed for a moving transmitter and also experimentally verified using the GLONASS satellite. Comparison between the satellite image and image obtained with imitator showed high level of similarity, suggesting the system is functioning properly.

A number of assumptions were made for developing the imaging algorithm. Our future work will focus on developing a generic algorithm and also experimentally evaluating the power budget and resolution of the SS-BSAR system.

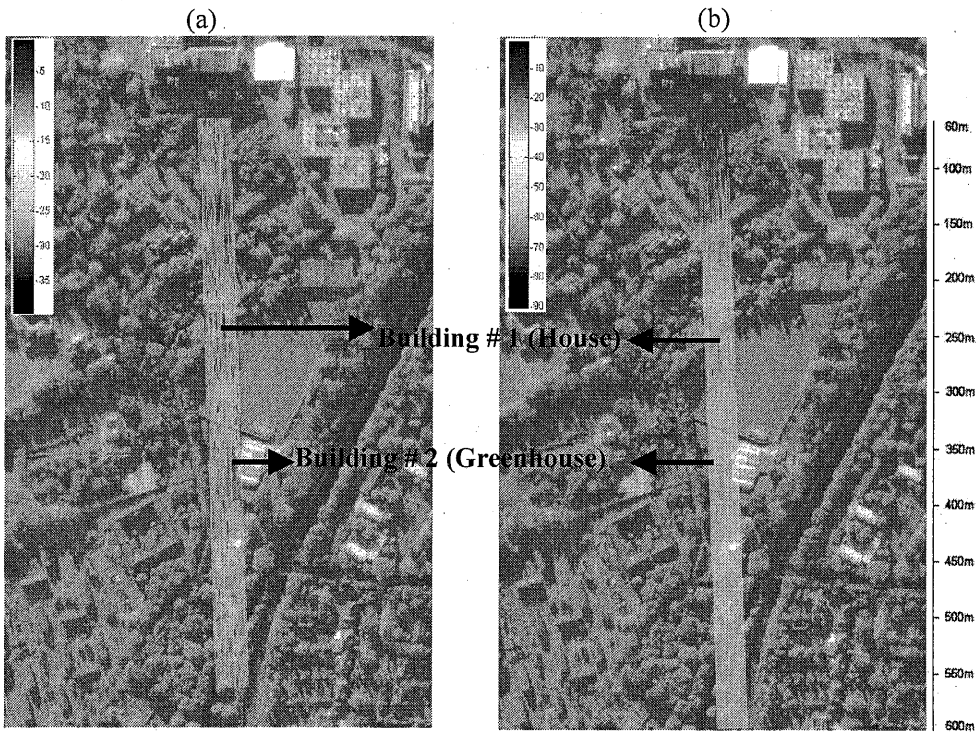

Figure 6: (a) Satellite image (b) Satellite signal imitator image

4 REFERENCES

1. M. Cherniakov., 'Space–surface bistatic synthetic aperture radar-prospective and problems', Proc. Int. Conf RADAR-2002, 22-26. Edinburgh (2002).
2. T.Zeng, M.Cherniakov,L.Teng, 'Generalized approach to resolution analysis in BSAR', IEEE transactions on Aerospace and Electronic Systems, 41(2), 461-474 (2005)
3. X.He,M.Cherniakov,T.Zeng, 'Signal detectability in SS-BSAR with GNSS non-cooperative transmitters', IEE Proceedings Radar, Sonar and Navigation. 152(3) , 124-132 (2005).
4. M.Cherniakov, R.Saini,R.Zuo,M.Antoniou, 'Bistatic synthetic aperture radar(BSAR) with transmitters of opportunity', Journal of Defence Science, 10(3), 136-140 (2005).
5. M.Cherniakov, R.Saini, M.Antoniou,R.Zuo,J.Edwards,'SS-BSAR with transmitter of opportunity-Practical aspects ' 3rd EMRS DTC Technical Conference, Edinburgh (2006).

ACKNOWLEDGEMENTS

The work reported in this paper was funded by the Electro-Magnetic Remote Sensing (EMRS) Defence Technology Centre, established by the UK Ministry of Defence and run by a consortium SELEX Sensors and Airborne Systems, Thales Defence, Roke Manor Research and Filtronic.